Robotica (2022), **40**, pp. 234–249
doi:10.1017/S0263574721000485

CAMBRIDGE
UNIVERSITY PRESS

RESEARCH ARTICLE

Tele-operation of an industrial robot by an arm exoskeleton for peg-in-hole operation using immersive environments

Sachin Kansal[1]*, Mohd Zubair[2], Bhivraj Suthar[2] and Sudipto Mukherjee[3]

[1]Computer Science Engineering Department, Thapar Institute of Engineering Technology, Patiala, Punjab, India, [2]Mechatronics Engineering Department, Chungnam National University, Daejeon, South Korea and [3]Mechanical Engineering Department, Indian Institute of Technology Delhi, New Delhi, India
*Corresponding author. Email: sachinkansal87@gmail.com

Received: 6 February 2020; **Revised:** 20 February 2021; **Accepted:** 2 April 2021; **First published online:** 14 May 2021

Keywords: tele-operation; remoting; KUKA KR5; immersive environment; Kalman estimation

Abstract

The design and development of an upper limb exoskeleton are being discussed for the tele-operation in order to control the KUKA KR5 industrial robot. When sufficient resolution is not provided by the visual feedback, feedback of haptic provides a qualitative understanding of changes in the remote conditions. This also provides tactile feedback from the virtual and real environment. Peg in a hole operation using exoskeleton works as the master for tele-operation in order to control the robot using immersive environment as visual feedback for the operator. The application of this work can be implemented as a nuclear power generation plant.

1. Introduction

Recent advances in actuators, sensors, materials, batteries, and computer processors have given new hope to creating the exoskeletons of yesteryear's science fiction. While the most common goal of an exoskeleton is to provide superhuman strength or endurance, scientists and engineers around the world are building exoskeletons with a wide range of diverse purposes.

Tele-operation process handles the machine from a distance. It is useful in hazardous environments, or where it is difficult for human to work, as the outer space, inside a nuclear power plant, or underwater due to the safety concerns, tele-operated robots are required [1]. It is advantageous to install robots in such locations. The motions of the robot have been superintended by operators (masters) which are situated at a safe place from menace centers. It is useful apparently in innocuous problem like fitting a peg in a hole. It has been possible to happen task planning systems work the same as the human brain; tele-operation makes a unified approach to handle precise applications. In previous papers, there have been triumphant executions of exoskeleton [1, 2, 3, 4]. Figure 1 shows the tele-operation of the real robot in remote maintenance and exploration to the virtual reality in virtual training. It consists of a total of seven joints from the wrist to the shoulder, having an adjustable length of the links that allow a correct alignment with the human joints [5, 6]. The total weight of the system is 3.5 kg and mainly comprises of aluminum structure and the actuators. In paper [7], presented a novel two hand gesture-based interaction technique for three-dimensional (3D) navigation in virtual environments (VEs). The proposed technique also allows users to efficiently control speed during navigation. The proposed technique is implemented via a VE for experimental purposes. In paper [8], presented an interaction technique where manipulation is performed by the perceptive gestures of the two dominant fingers: thumb and index. In paper [9], a low-cost exoskeleton for the elbow that is connected to a context-aware architecture is presented.

In VR system, the patient can perform rehabilitation exercises in an interactive way. The integration of virtual reality technology in rehabilitation exercises provides an intensive, repetitive, and task-oriented

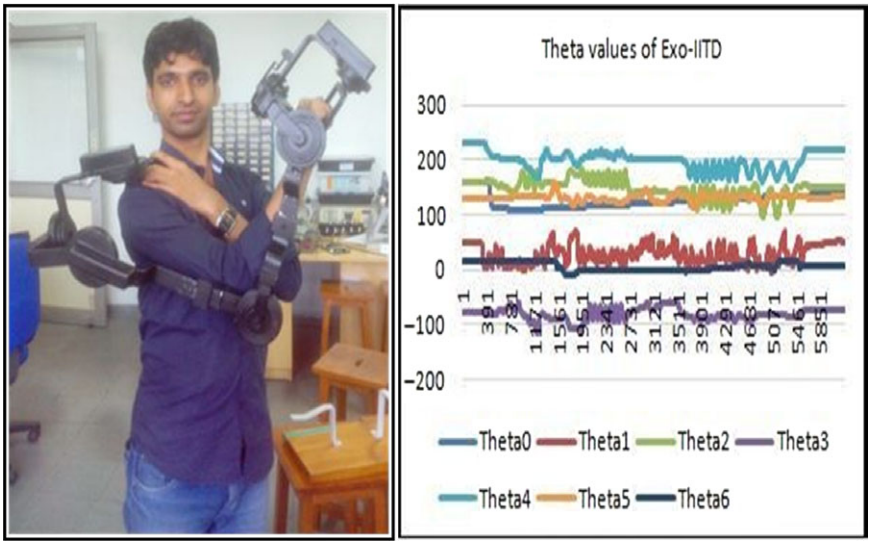

Figure 1. *Exoskeleton design and angles extraction (Theta0-Theta6) for the tele-operation.*

capacity to improve patient motivation and reduce work on medical professionals. The US military had developed several exoskeletons to augment and amplify the soldier ability for military purposes [10]. Then, the General Electric Company developed two-armed master–slave manipulator used for handling radioactive equipment. The master is an exoskeleton type robot worn by the operator and its motion was reproduced by the two-armed slave unit [11]. Moreover, the John Hopkins University designed the upper limb exoskeleton type to help elbow flexion of paralyzed people [12]. Almost at the same time, the Beograd anthropomorphic exoskeleton was designed for lower limb application [13]. The development of the exoskeleton has been increased in various implementations. Mechanical characteristic of the exoskeleton has been reviewed many times. Gopura et al. reviewed mechanical aspect of upper limb exoskeleton [14, 15], and Bogue et al discussed the recent development of the exoskeleton [16].

This control scheme was utilized to control seven degrees of freedom (DOF) upper limb exoskeleton to help the motions of shoulder vertical and horizontal flexion/extension, shoulder abduction/adduction, elbow flexion/extension, forearm supination/pronation, wrist flexion/extension, and wrist radial/ulnar deviation of physically weak individuals [17, 18].

1.1. Proposed method

The exoskeleton is a robotic arm aiming for building a complete tele-operation station, in which human operator wears an exoskeleton arm in order to control a virtual slave robot remotely, that is, KUKA KR5 manipulator as shown in Fig. 1. Various applications for this exoskeleton system, that is, from tele-operation of the real robot in the field of exploration to virtual reality, remote maintenance and in the domain of virtual training [19]. It consists of total of seven joints from the wrist to the shoulder, having an adjustable length of the links that allow a correct alignment with the human joints, as shown in Fig. 2.

1.2. Kinematic design

The work focuses on developing an arm exoskeleton to be worn by a human. It has been provided with the required information to control a commercial robot by hand motion from a certain distance. One of the applications of the exoskeleton is targeted peg-in-hole, which has been accomplished through

https://doi.org/10.1017/S0263574721000485 Published online by Cambridge University Press

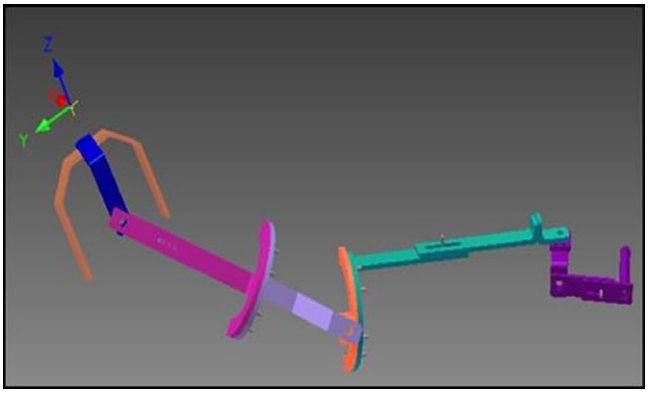

Figure 2. *An exoskeleton robot.*

Algorithm 1 Extracting voltage from the calibrated sensors and perform filtering in various stages, implementing the forward kinematics, estimation, communicating with the KUKA KR5 industrial robot.

Input: Voltage ([*n*]channels) [***Noise Removal Output***], *links length* ($\boldsymbol{d}_n$), *Joint offset* ($\boldsymbol{b}_n$), *Joint Angle* (θ_n)*[Joint Variable], Twist Angle* (α_n).

Initial*:* $\boldsymbol{n}$ *= 7 (Number of Joints)*

Output*: End-Effector Position of the exoskeleton EE[x], EE[y], EE[z] with respect to the base frame.*

Begin

for $\boldsymbol{i} \leftarrow$ ***1:*** $\boldsymbol{n}$

transformation Matrix = {{Cos(θ[n]), - Sin (θ [n]) * (α[n]), (θ[n]) * Sin(α[n]), $\boldsymbol{b}$[n] * Cos(θ) },{ Sin(θ[n]), (θ[n]) * Cos(α[n]),- Cos(θ[n]) * Sin(α[n]), $\boldsymbol{b}$[n] * Sin(θ[n]) },{ 0,Sin(α[n]), Cos(α[n]), d[n] }, { 0, 0, 0, 1 }};

End for Begin

Perform the Kalman Estimation for [X, Y, Z] axes respectively

Integration of the Exoskeleton and the immersive environment for performing the tele-operation.

End

Perform the conversion from position command to the velocity command and send to the KUKA controller

End Begin

a KUKA manipulator. The motion of end-effector of the exoskeleton is replicated in KUKA robot by power amplification for effective functioning.

The shoulder joint has three degrees of freedom, the elbow joint has two degrees of freedom, and the wrist joint has two degrees of freedom. Seven sensors are attached on the exoskeleton in order to capture the sense the variation of the joint angle. Tekscan's FlexiPot Potentiometers (Fig. 3) are used for shoulder joint and pronation–supination (twisting) of the elbow joint. Rotary Potentiometers (Fig. 4) are used for the measurement of the angle of rotation of flexion–extension (forward-backwards) and abduction–adduction (inside-outside) motions. The anthropometric exoskeleton has seven degrees of freedom, whereas the KUKA KR5 ARC has six degrees of freedom (shown in Fig. 5).

https://doi.org/10.1017/S0263574721000485 Published online by Cambridge University Press

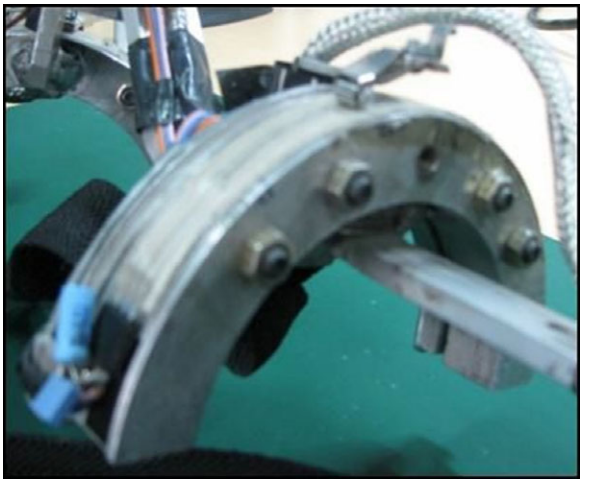

Figure 3. *FlexiPot potentiometers.*

Figure 4. *Rotary Potentiometers.*

1.2.1. Inverse kinematics

The DOF varies in the master device (exoskeleton) and the slave device (KUKA KR5); therefore, one-on-one mapping is not possible here. The KUKA KR5 has invariant kinematics, whereas exoskeleton has a function to adjust the length of the link to allow couture based on the operator's arm size. Firstly, computes position and orientation of the lateral end of the exoskeleton from the sensor readings, it matches the position and orientation of the arm tip to the position of the manipulator's end-effector.

The positions and orientations of the joint that the KUKA must retrieve to reinvigorate the same posture are calculated through the known posture of the end-effectors. This is inverse kinematics process. The solution is not unique for inverse kinematics and has to be punctiliously handled for stability and physical feasibility.

1.2.2. Remoting

The exoskeleton and KUKA can be run on a single system, but this may lead to the problem of communication wires. Two systems are used here, one to quantify the forms of kinetics made by the exoskeleton and the other to the controller of the KUKA. The .NET remoting has been utilized for such a system.

https://doi.org/10.1017/S0263574721000485 Published online by Cambridge University Press

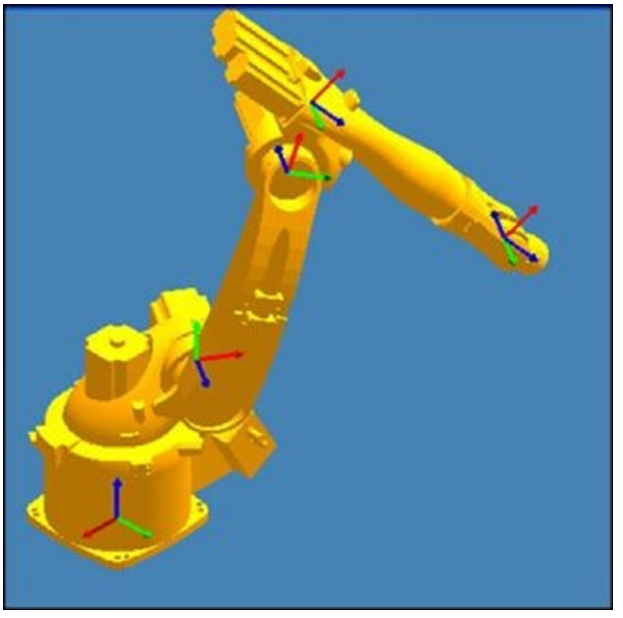

Figure 5. *KUKA CAD Model.*

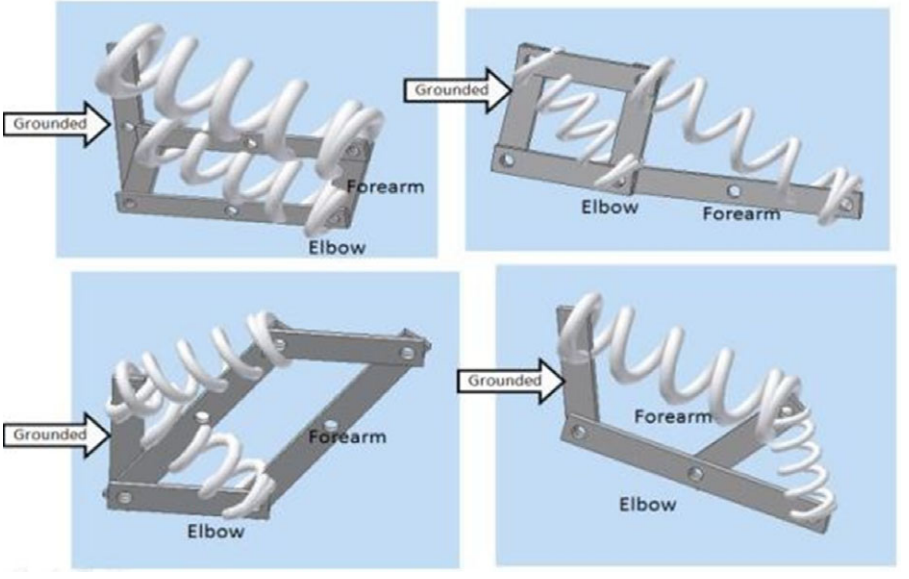

Figure 6. *Four possible configurations for two-link mechanisms at the wrist.*

1.2.3. Gravity balancing

Each brake is of 400-g weight. It exerts significant shear on the operator upon perpetuated exposure. Gravity loading without scarifying dynamic performance can be done by spring-based gravity balancing method [20]. The selection of the points of attachments of the springs is important such that the variation having a change in process configuration becomes zero. The exoskeleton has done gravity balance through two brakes at the wrist joint. Figure 6 displays four possible configurations to investigate it for them system designed as 2 planar link problem. The configuration that was selected finally is shown in Fig. 7 below.

https://doi.org/10.1017/S0263574721000485 Published online by Cambridge University Press

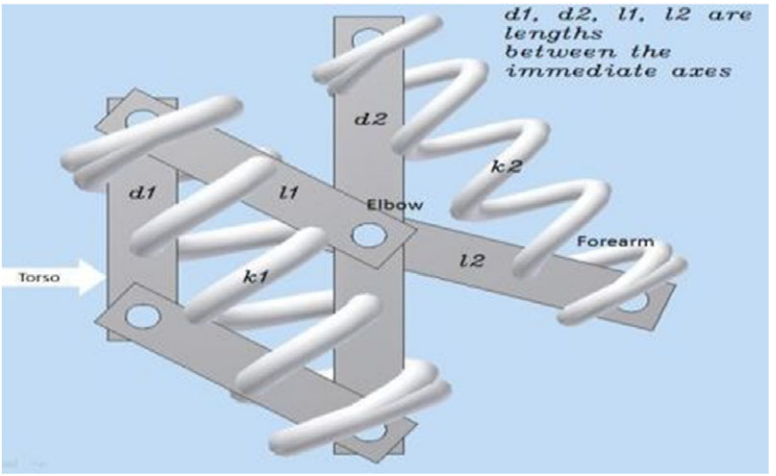

Figure 7. *Gravity balancing mechanism.*

There is no limit for selection of d1 and d2 values, let assume d1 = d2, then springs having similar spring constant and which is easier than finding two different types of springs. M is the mass of two brakes at the wrist (0.8 kg) including half of the mass of exoskeleton without the brakes (0.6 kg), that is, M = 1.4 kg. The primary criteria for selecting a spring have been the available extension, which is of the order of 0.5 m. One such spring is LEM080BB05 having natural length 290 mm, maximum extended length 515 mm, and spring constant 110 Newton/m.

1.3. Kalman filter estimation for each of the axes

The motion of the human limb being sensed by the exoskeleton is observed to be noisy. There is a significant amount of jittering observed even when the exoskeleton is maintained static, and no motion input is provided. This causes the KUKA to respond to the exoskeleton's state through a visibly notable vibration. Once forward kinematics has been performed, the end-effector position is then estimated using Kalman filter in each axes and then mapped to the KUKA after converting into the velocity mode.

This algorithm has two-step process, predict and update. In the prediction step, approximate of the current state variables and their suspicion are engendered from the Kalman filter. In the updating step, the outcome of the next quantification (compulsorily corrupted with some amount of error, including arbitrary noise) is observed and updates these approximate. This algorithm is recursive in nature. This utilizes the present input quantifications and the previously calculated state only, and its suspicion matrix in real-time. The Kalman filter approximates the internal state of a linear dynamic system from a series of noisy quantification recursively.

In order to implement a Kalman filter, the process needs to be framed in accordance with the Kalman framework. Pre-requisites:

F_k: the state-transition model;
H_k: the observation model;
Q_k: the covariance of the process noise;
R_k: the covariance of the observation noise; and
B_k: the control-input model (for simple systems, this can be omitted) for each time-step, "k."

The Kalman filter surmises the true state at time k has evolved from the state at (k – 1) according to

$$x_k = F_k x_{k-1} + B_k u_k + w_k$$

https://doi.org/10.1017/S0263574721000485 Published online by Cambridge University Press

where F_k is the state transition model which has been applied to the previous state x_{k-1}; it takes every point in our original estimate and moves it to a new predicted location, which is where the system would move if the original estimate was correct.

B_k is the control-input model which is applied to the control vector u_k. It defines the external factors affecting the system.

w_k is the process noise which is surmised to be drawn from a zero-mean normal distribution with covariance ^{Q}k. This noise accounts for external uncertainties (unknown factors), which affects the state of the system, but are not considered in the model. Thus, the un-tracked influences are considered as noise with covariance ^{Q}k.

$$w_k \sim \mathcal{N}(0, Q_k)$$

The initial state, x_k, is a random vector with known mean $\mu 0 = E(x0)$ and covariance P0 = E((x0−μ0) (x0−μ0)^{T}). At time k, an observation (or measurement) z_k of the true state x_k is made according to

$$z_k = H_k x_k + v_k$$

where H_k is the measurement model which models the sensors which give us information about the state of the system and v_k is the quantification noise which is surmised to be zero-mean Gaussian white noise with covariance R_k. The measurement noise is the sensor noise, which defines the uncertainty in the state as measured by the sensors.

$$v_k \sim \mathcal{N}(0, R_k)$$

The Kalman filter has two distinct phases: predict and update. The algorithm steps are shown below.

Predict

Predicted (a priori) state estimate
$xk|k-1 = Fkx_{k-1|k-1} + Bkuk$
Predicted (a priori) estimate covariance $P_{k|k-1} = F_k P_{k-1|k-1} F_k^T + Q_k$

Update

Innovation or measurement residual $\hat{y}_k = z_k - H_k \hat{x}_{k|k-1}$
Innovation (or residual) covariance $S_k = H_k P_{k|k-1} H_k^T + R_k$
Optimal Kalman gain $K_k = P_{k|k-1} H_k^T S_k^{-1}$
Updated (a posteriori) state estimate

$$\hat{x}_{k|k} = \hat{x}_{k|k-1} + K_k \tilde{y}_k$$

Updated (a posteriori) estimate covariance $P_{k|k} = (I - K_k H_k) P_{k|k-1}$

Real-time results:
The Kalman filter algorithm was implemented in real-time, considering a single axis at a time. The actual measurements are as depicted in blue (showing jitter), and the Kalman estimation is as shown in red (Figs. 8–10) representing X, Y, Z axis, respectively.

1.4. Haptics: Exoskeleton's tele-operation of industrial robot

A qualitative understanding of transmutations in the remote environment with exoskeleton happened by haptic feedback. It will help especially when visual feedback does not have sufficient resolution value. As in this module of exoskeleton design, the target is to use the reaction forces sensed by KUKA KR5 to guide peg insertion tasks. This haptic device provides tactile feedback from the real or VE to a human operator for performing peg in a hope operation. The target is to use the reaction forces sensed by an industrial manipulator to guide peg insertion tasks. Realization of a haptic interface provides tactile feedback from the real or VE to a human operator for tele-operation. An upper limb haptic exoskeleton

https://doi.org/10.1017/S0263574721000485 Published online by Cambridge University Press

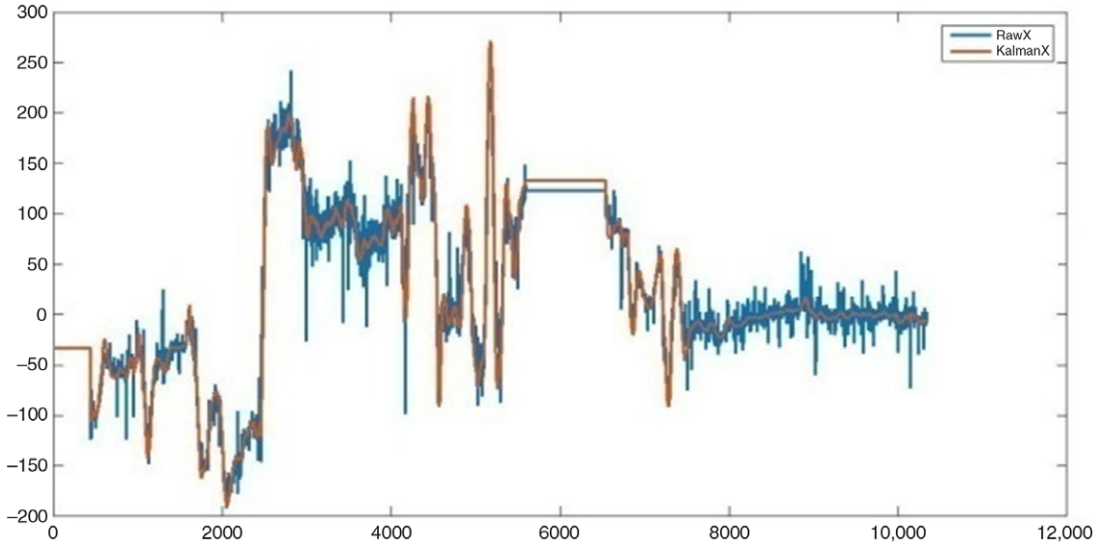

Figure 8. *Real-time results for raw exoskeleton versus Kalman estimation in X-axis.*

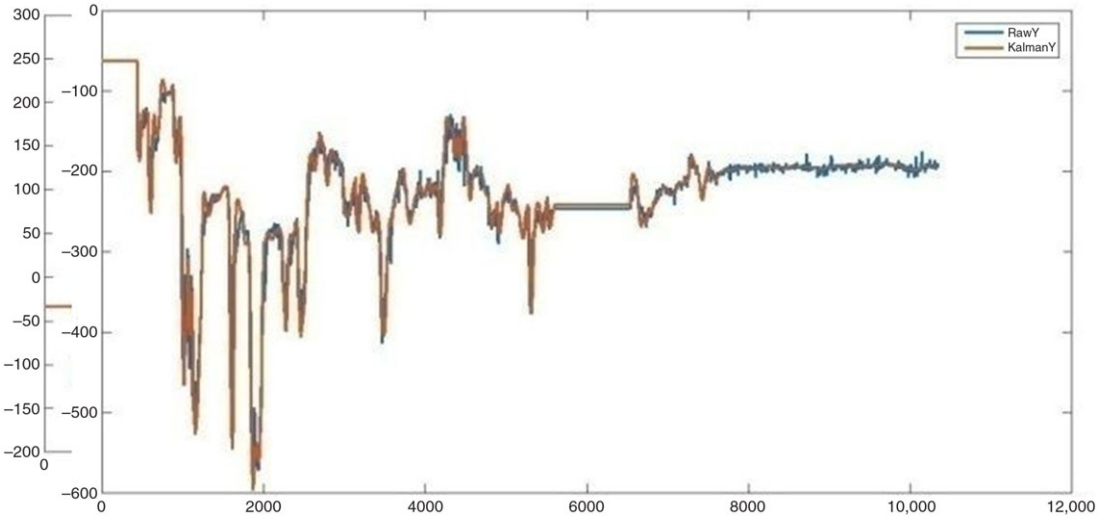

Figure 9. *Real-time results for raw exoskeleton versus Kalman estimation in Y-axis.*

has been designed to use as a master for tele-operation designed to control a conventional industrial manipulator. The magnitude of haptic feedback is intended to be reflective of and not exactly the same as the torques seen in actual operation. This is an exemplar technology in reflecting the remote manipulator forces and torque to the operator by the exoskeleton. Torque to current is almost linear in an electro-mechanical brake, as shown in Fig. 11. In a magnetic particle brake, torque can be controlled very accurately. The magnetic flux tries to bind the particles together when the electricity is applied to the coil. As the electric current has been incremented, the binding of the particles becomes more vigorous. The brake rotor passes through these bound particles. As the particles start to bind together, a resistant force has engendered on the rotor, slowing, and eventually ceasing the output shaft.

The input is free to turn with the shaft when electricity is removed from the brake. Brakes which are used for haptic, has weighed of about half a kilogram, can exert strain on the wearer upon perpetuated exposure.

https://doi.org/10.1017/S0263574721000485 Published online by Cambridge University Press

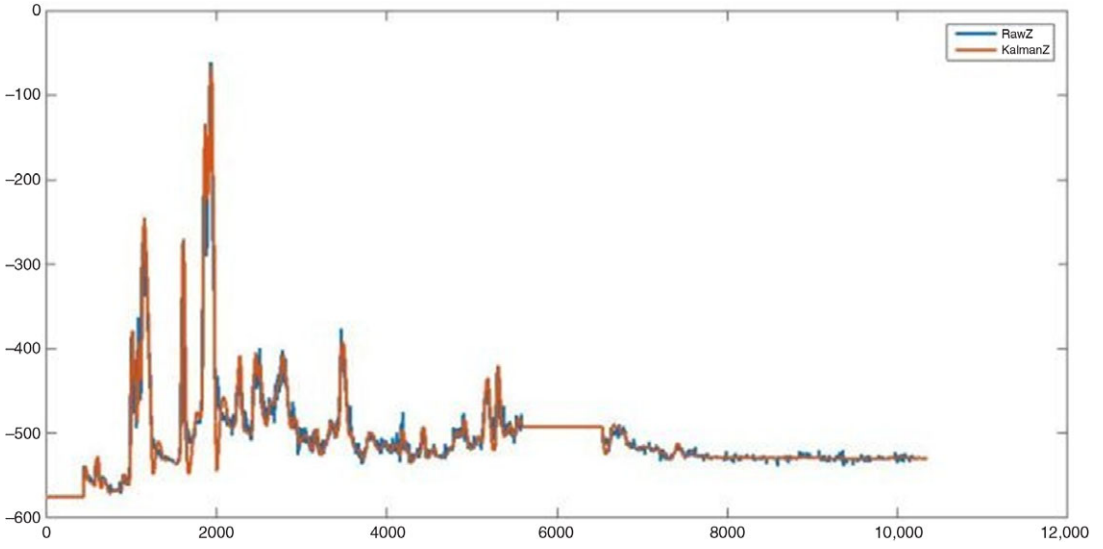

Figure 10. *Real-time results for raw exoskeleton versus Kalman estimation in Z-axis.*

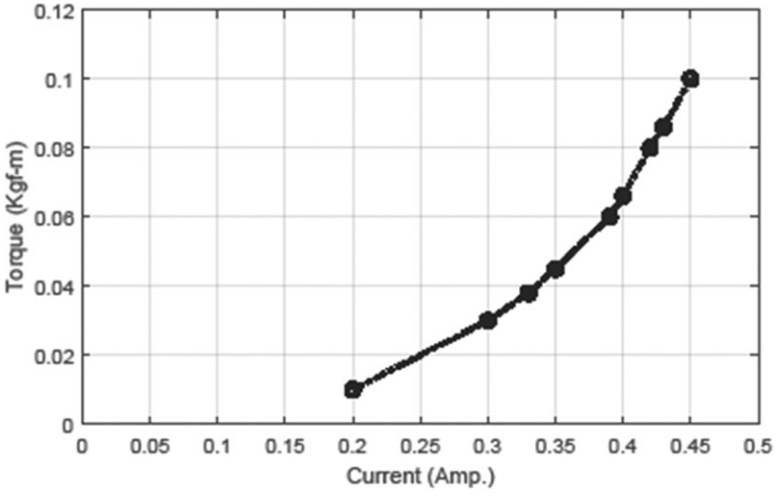

Figure 11. *Performance of PMB-10.*

1.5. Mapping of exoskeleton with the virtual KUKA robot (2D view)

An Autodesk inventor model of the exoskeleton arm and the KUKA robot is clubbed together to a VE. The exoskeleton replicated motion is being reflected by the KUKA virtual model (2D view). One-to-one mapping between the virtual exoskeleton and KUKA manipulator models is performed, whenever the operator performs motion in the exoskeleton. Each iteration of the exoskeleton joint angle is reflected in its model along with the corresponding state of the KUKA model.

Firstly, computes pose of the distal terminus of the master from the sensor readings to map the pose of the hand tip to the position of the manipulator's terminus effector. This is called computing the forward kinematics in robotics terminology performed by successive matrix computations. Once the instance of the exoskeleton end-effector has been kenned, the pose that the KUKA has to achieve is evaluated by inverse kinematic.

https://doi.org/10.1017/S0263574721000485 Published online by Cambridge University Press

For evaluating inverse kinematics, we can treat the center of rotation of wrist as the end-effector since we know its position and orientation. Its orientation is the same as that of the tool. The rotation of the first three joints of the robot is basically responsible for the positioning of the end-effector of the robot. The first three joints and links of the robot behave as a three-link manipulator. Geometry can be used to calculate these three angles given the position of the end-point of the third link. The next three joints are responsible for the orientation of the end-effector. These angles can be calculated using matrix manipulation. If the position of the tool is given to us rather than the position of the center of rotation of wrist, then we can use the following equations to reach the center of rotation of wrist (p_x, p_y, p_z). Let the position of tool be (p_x^t, p_y^t, p_z^t), then

$$p_x = p_x^t - d_6 a_x - a_6 n_x$$
$$p_y = p_y^t - d_6 a_y - a_6 n_y$$
$$p_z = p_z^t - d_6 a_z - a_6 n_z$$

After calculating these values, we can treat the center of rotation of wrist in our calculations as the end-effector. The center of rotation of wrist will be referred to as the end-effector in this article. We are using the center of rotation as the end-effector simplifies our calculations and allows us to decouple the wrist from the first three joints. The rotations of the first three joints only are replication for the position of the end-effector as already discussed.

The origin of frames 0–5 is fixed such that all of them lie in one plane (which is perpendicular to the x-y plane of frame 0 and contains the z-axis of frame 0). The origin frames 4 and 5 lie at the center of rotation of the wrist. An imaginary line joining origin of frame 0 and frame 4 always revolves around the z-axis. Hence from the top view of the robot, it can be inferred that.

Let the position of end-effector in frame 1 be:

$$\tan\theta_1 = p_y/p_x$$

Thus, $\theta_1 = \tan^{-1}(p_y/p_x)$

Let the position of end-effector in frame 1 be: (p_x^1, p_y^1, p_z^1)

We can treat frame 1 to frame 2 as one link and frames 2–4 as the second link of a two-link manipulator. Since the rotation of the fourth joint does not affect the position of end-effector, we can assume the second link of a two-link manipulator to be from frames 2–4. Thus, if l_1 and l_2 are the link lengths of the two link manipulator and (x, y) is the position of the end-effector of the two link manipulator.

$$l_1 = a_2,\ l_2 = \sqrt{a_3^2 + d_4^2},\ x = p_x^1, y = p_y^1,$$

If α and β are the angles made by the links of a two-link manipulator, then:

$$x = l_1 \cos\alpha + l_2 \cos(\alpha + \beta)$$
$$y = l_1 \sin\alpha + l_2 \sin(\alpha + \beta).$$

Squaring and adding the above two equations

$$x^2 + y^2 = l_1^2 + l_2^2 + 2l_1 l_2 \cos\alpha \cos(\alpha + \beta) + \sin\alpha + \sin(\alpha + \beta)$$

$$\cos\beta = \frac{x^2 + y^2 - (l_1^2 + l_2^2)}{2l_1 l_2}.$$

Two values of β are possible while taking the cosine inverse, having the same magnitude but opposite sign. We select the elbow down solution, that is, the value for which the configuration of KUKA is esthetically similar to that of the human arm.

https://doi.org/10.1017/S0263574721000485 Published online by Cambridge University Press

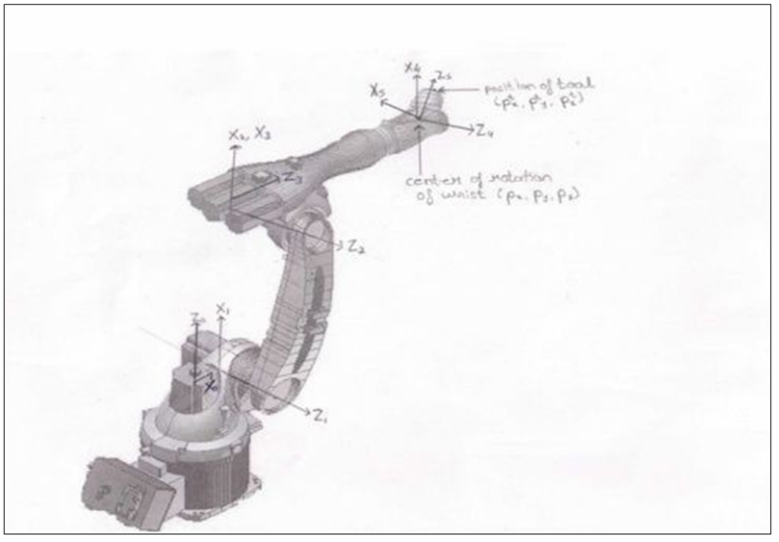

Figure 12. *KUKA robot with DH frame attached for evaluating inverse kinematic solution.*

Substitute values of β in x and y equations and expand to get:

$$x = l_1\cos\alpha + l_2\cos\alpha\cos\beta - l_2\sin\alpha\sin\beta$$
$$x = (l_1 + l_2\cos\beta)\cos\alpha - (l_2\sin\beta)\sin\alpha$$
$$y = (l_2\sin\beta)\cos\alpha + (l_1 + l_2\cos\beta)\sin\alpha.$$

The above two simultaneous equations in $\cos\alpha$ and $\sin\alpha$ can be solved uniquely for $\cos\alpha$ and $\sin\alpha$. So, α is known uniquely for a value of β.

$$\alpha = \text{atan2}(\sin\alpha, \cos\alpha);$$
$$\alpha = \tan^{-1}\left(\frac{y\,(l_1+l_2\cos\beta\,) - xl_2\sin\beta}{yl_2\sin\beta + x(l_1+l_2\cos\beta)}\right)$$

where α is the angle of link 1 with the ground and β is the angle of link 2 with link 1.

Hence, $\theta_3 = \cos^{-1}\cos\beta + \tan^{-1}(d_4/a_3)$

$\tan^{-1}(d_4/a_3)$ is added to align the link to its zero position. Due to workspace limitations, θ_3 is always negative, but the function $\cos^{-1}(\beta)$ will give a positive value. Hence, a minus sign is incorporated to express θ_2.

$$\theta_2 = \tan^{-1}\tan\alpha - \pi/2$$

Let A_1 denote the matrix expressing position and orientation of frame 1 with respect to the frame 0. Similarly, A_2 denotes the matrix expressing position and orientation of frame 2 with respect to the frame 0. And A_i^{i-1} denotes the position and orientation of frame i with respect to the frame i-1. A_6 denotes the position and orientation of the end-effector of the robot with respect to the frame 0 (i.e. ground). The inverse kinematics (shown in Fig. 12) is invariant and tricky as the solution is not unique and to be meticulously managed for stability and physical feasibility.

Figure 13 shows the application windows. Windows form at the lower right corner contains several buttons that either increment or decrement each of the 7 exoskeleton joint angles. Whereas the "Reset" button brings the exoskeleton position to that which a human arm attains once it is lowered straight.

https://doi.org/10.1017/S0263574721000485 Published online by Cambridge University Press

Figure 13. *Manual input to exoskeleton for KUKA replication.*

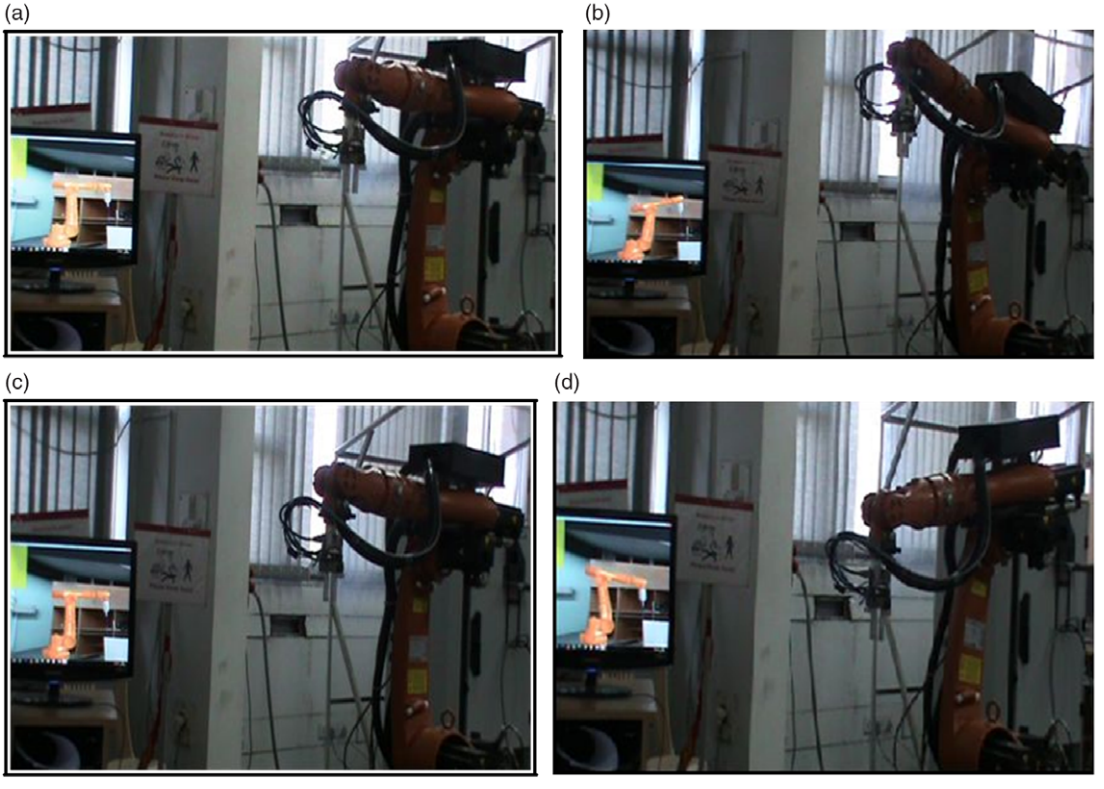

Figure 14. *(a–d). Immersive environment interaction (real, augmented reality environment KUKA and real exoskeleton) (a–b: KUKA moving upward in real and immersive), (c–d: KUKA moving downward in real and immersive).*

https://doi.org/10.1017/S0263574721000485 Published online by Cambridge University Press

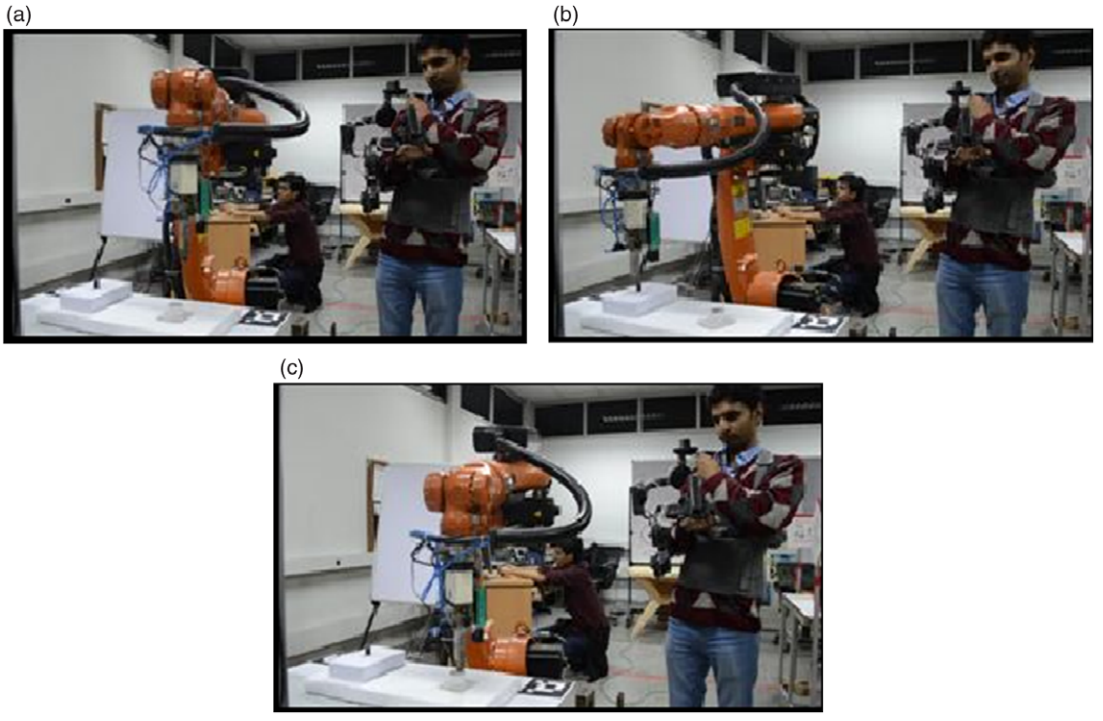

Figure 15. *(a–c). Peg in a hole operation by KUKA using exoskeleton (real KUKA and real exoskeleton).*

1.6. Tele-operation of KUKA KR5 by an arm exoskeleton through immersive environment for peg-in-hole operation (3D view)

The overall concept of the immersive environment development is to avoid the operator to be present in the dangerous, dirty, dull environments, and the operator can perform the tele-operation from a safe distance. Likewise, various surgical robot (da Vinci robot) [21, 22] is used for performing minimally invasive surgery from a remote distance (operators are surgeons). They also use 3D mapping technology in order to see the region of interest (surgical area) in great detail that too in real-time scenarios.

Peg in a hole operation utilizing an upper arm exoskeleton is being used as a master for performing tele-operation in order to control industrial robot (KUKA). The KUKA robot is acting as a slave using immersive environment as visual feedback for the operator. Communication between the sub-systems is achieved using the UDP protocol forming a closed-loop exchange of parameters (between real KUKA, exoskeleton, and the immersive KUKA environment).

The exoskeleton application determines the mapping between the six angles of the KUKA and the seven angles of the exoskeleton. Then it sends the calculated values of the six angles; using these, we animate the model of the KUKA in our application, as shown in Fig. 14(a-d).

Host to KUKA direct communication protocol has been implemented. In order to test one-on-one communication, console-based application was developed and tested directly with the KUKA, as shown in Fig. 15(a-c). The operator will insert peg in hole via immersive environment as visual feedback, and the immersive KUKA also got updated to have the latest status of the joint angles.

2. Result

In Fig. 16, mapping between the exoskeleton and KUKA is performed while doing the tele-operation.

https://doi.org/10.1017/S0263574721000485 Published online by Cambridge University Press

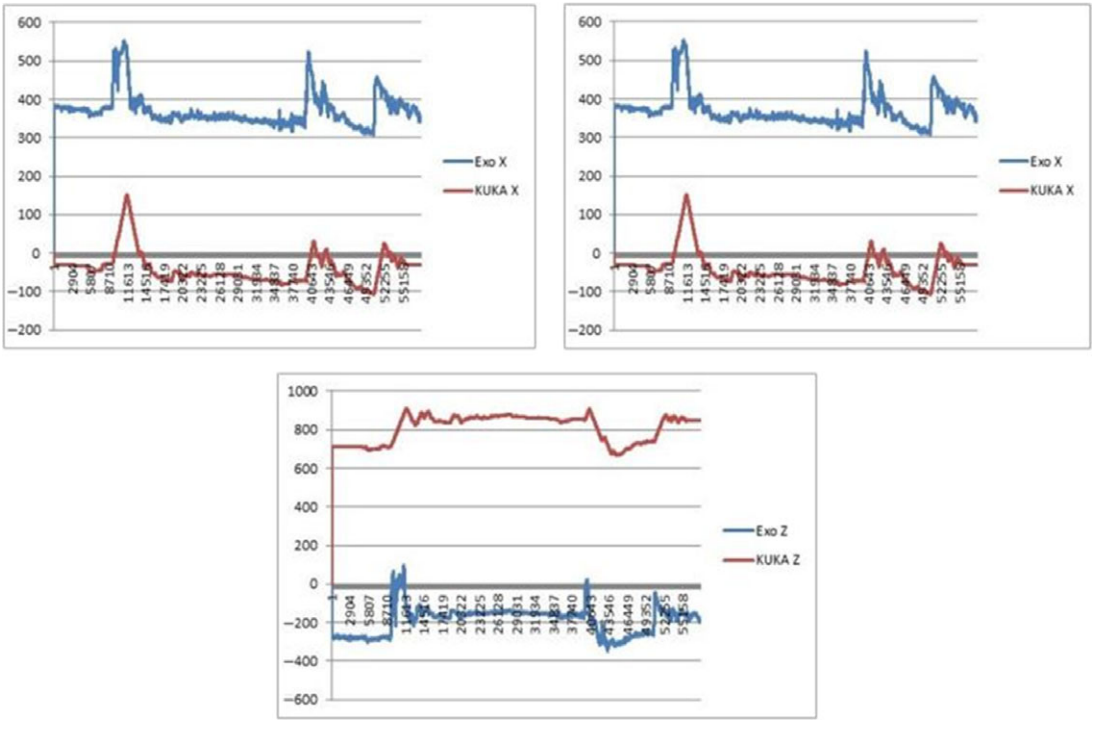

Figure 16. *Exoskeleton and KUKA mapping in X, Y, Z-axis, respectively.*

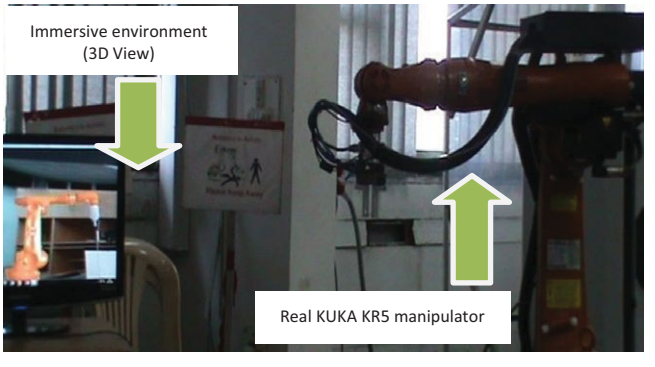

Figure 17. *Integrating exoskeleton, real KUKA, and immersive environment virtual KUKA.*

In Fig. 17, tele-operation of the KUKA robot using the exoskeleton via immersive-based environment is performed, and Fig. 18 represents the CAD model of the designed exoskeleton for performing the tele-operation using the VEs in real-time scenario.

3. Conclusion and future work

We performed the tele-operation of the KUKA KR5 industrial robot by the exoskeleton via immersive environment and using Kalman-based position estimation. We selected I^2C communication architecture to take full advantages of 2-wire serial bus. Two various modes of operation are also reported, that is, position scaling and velocity scaling solution. The jitter is of the order 2–3 mm present in the system

https://doi.org/10.1017/S0263574721000485 Published online by Cambridge University Press

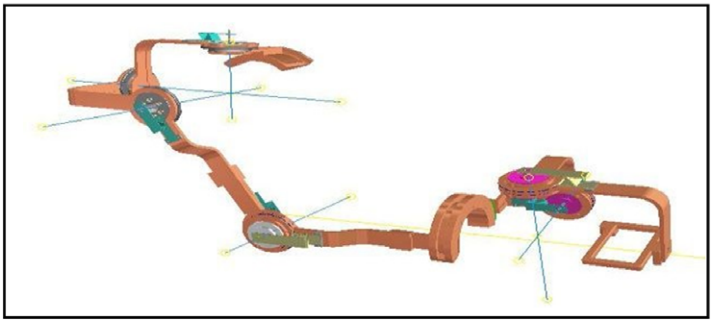

Figure 18. *CAD model of exoskeleton.*

which is dynamic in nature. In order to do the peg in hole operation remotely, the immersive environment is created so that the 3D view can be achieved for the operator. The overall idea for the development of the immersive environment is to refrain the operator from the highly radioactive environment, and through this experiment, the operator can perform the tele-operation of the industrial robot using the exoskeleton from a safe distance in the real-time scenario.

Acknowledgment. We hereby acknowledge support of the BRNS is acknowledged for providing the environment for carrying out the activity.

References

[1] K. Kiguchi, S. Kariya, K. Watanabe, K. Izumi and T. Fukuda, "An exoskeleton robot for human elbow motion support – sensor fusion, adaptation and control," *IEEE Trans Syst Man Cybern*. **31**, 353–361 (2001).
[2] C. Lin, J. H. Goldberg and A. Freivalds, "A non-exoskeleton optoelectric wrist goniometer," *Int J Ergon*. **11**(3), 233–242 (1993).
[3] Y. Chen, J. F. Zhang, C. J. Yang and B. Niu, "Design and Hybrid Control of the pneumatic force-feedback systems for Arm-Exoskeleton by using on/off valve," *Mechatronics*. 325–335 (2007) http://dx.doi.org/10.1016/j.mechatronics.2007.04.001
[4] M. Bergamasco, B. Allotta, L. Bosio, L. Ferretti, G. Parrini, G. M. Prisco, F. Salsedo and G. Sartini, "An arm exoskeleton system for tele-operation and virtual environments applications," *IEEE Int Conf Robot Autom*. **2**, 1449–1454 (1994).
[5] S. Mukherjee, M. Zubair, B. Suthar and S. Kansal. "Exoskeleton for tele-operation of industrial robot," pp. 1–5, AIR '13 Advances In Robotics 2013, Pune, India July 04–06, ACM New York, NY, USA ©2013, Copyright 2013 ACM 978-1-4503-2347-5/13/07, (2013). http://dx.doi.org/10.1145/2506095.2506108.
[6] S. Mukherjee, B. Suthar, S. Kansal and M. Zubair, "Closed loop autonomous calibration of tele-operation exoskeleton exoskeleton for tele-operation of industrial robot," AIR '13 Advances In Robotics 2013, Pune, India — July 04–06 (2013).
[7] I. Rehman, S. Ullah and M. Raees, "Two hand gesture based 3D navigation in virtual environments," *Int J Interact Multi Artif Intell*. **5**(4), 128–140 (2018).
[8] M. Raees and S. Ullah, "GIFT: Gesture – based interaction by fingers tracking, an interaction technique for virtual environment," *Int J Interact Multi Artif Intell*. **5**(5), 115–125 (2018).
[9] D. Iglesia, A. Mendes, G. Gonzalez, D. Bravo and J. Sanatana, "Connected elbow exoskeleton system for rehabilitation training based on virtual reality and context-aware," in Sensors Journal, MDPI (2020).
[10] W. Cloud, "Man amplifiers: Machines that let you carry a ton," *Popul Sci.* **187**(5), 70–73 & 204 (1965).
[11] R. S. Mosher and S.o.A. Engineers, Handyman to Hardiman: Society of Automotive Engineers (1967).
[12] G. Schmeisser and W. Seamone, "An upper limb prosthesis-orthosis power and control system with multi-level potential," *J Bone Joint Surg (Am).* **55**(7), 1493–1501 (1973).
[13] M. Vukobratovic, D. Hristic and Z. Stojiljkovic, "Development of active anthropomorphic exoskeletons," *Med Biol Eng Comput*. **12**(1), 66–80 (1974).
[14] R. A. R. C. Gopura and K. Kiguchi, "Mechanical designs of active upper-limb exoskeleton robots: State-of-the-art and design difficulties," IEEE International Conference on Rehabilitation Robotics (ICORR) (2009).
[15] R. A. R. C. Gopura, K. Kiguchi and D. S. V. Bandara, "A brief review on upper extremity robotic exoskeleton systems," 6th IEEE International Conference on Industrial and Information Systems (ICIIS) (2011).
[16] R. Bogue, "Exoskeletons and robotic prosthetics: a review of recent developments," *Ind Rob: Int J*. **36**(5), 421–427 (2009).

[17] R. A. R. C. Gopura, K. Kiguchi and L. Yang, "SUEFUL-7: A 7DOF upper-limb exoskeleton robot with muscle-model-oriented EMG-based control," IEEE/RSJ International Conference on Intelligent Robots and Systems (IROS). (2009).
[18] K. Kiguchi and Y. Hayashi, "An EMG-Based control for an upper-limb power-assist exoskeleton robot," *IEEE Trans Syst Man Cybern Part B.* PP(99), 1–8 (2012).
[19] V. Abbasi, B. Azria, E. Tabarah, V. Menon and M. Bedirian, "Improved 7-DOF control of ISS robotic manipulators," Proc 8th Int Conf Space Operations. (2004).
[20] S. K. Agrawal and A. Fattah, "Gravity balancing of a spatial robotic manipulator," *Mech Mach Theor.* **39**(1), 1331–1344 (2004).
[21] https://en.wikipedia.org/wiki/Da_Vinci_Surgical_System.
[22] N. Bulgaria, A. Sen, P. Kalra and S. Kumar, "Immersive environment for robotic tele-operation," in AIR '15 Advances In Robotics 2015, Goa, India — July 02–04 (2015).

Cite this article: S. Kansal, M. Zubair, B. Suthar and S. Mukherjee (2022). "Tele-operation of an industrial robot by an arm exoskeleton for peg-in-hole operation using immersive environments", Robotica **40**, 234–249. https://doi.org/10.1017/S0263574721000485